A SEISMIC WAVE GUIDE PHENOMENON*

K. E. BURG,† MAURICE EWING,‡ FRANK PRESS,‡ E. J. STULKEN†

ABSTRACT

On one particular prospect in shallow water repetitive patterns appeared on short spread seismograms in such prevalence as to jeopardize identification of desired reflections. It is demonstrated that under favorable conditions, less restrictive than thought necessary heretofore, a layer of water comprises an effective wave guide for seismic energy propagation. Reinforcement fronts formed by multiple reflection of sound in water can develop into a set of waves completely overshadowing other seismic arrivals. With but minor modifications conventional wave guide theory applies.

Examples from the prospect are presented to illustrate various reinforcement patterns. Observed frequency characteristics, group velocity, and phase velocity magnitudes are investigated for normal modes of propagation.

INTRODUCTION

Oil prospecting over water has revealed sound transmission characteristics either absent or less obvious on land. Among these can be mentioned repeated bursts of energy traceable to oscillations of the explosion bubble, simple multiple reflections between bottom and surface of the water, offside reflections from objects near the surface, and wave guide propagation which usually involves dispersion.

This last characteristic, wave guide propagation, stems from reflections between top and bottom of the water layer. The high frequency of first energy arrivals associated with long range direct waves in shallow water comprises one manifestation. Seismic observations reveal that this initial high frequency wave marks the beginning of a band of waves whose frequency rapidly decreases. These waves of continuously lower frequency persist until terminated by the Airy phase. The theory for the case of a liquid bottom has been given by Pekeris and for a solid bottom by Press and Ewing. In both these cases the propagation is due to total reflection within the liquid layer involving rays whose angle of incidence at the bottom lies between the critical angle and the grazing angle.

In this paper we deal with a closely related phenomenon involving more nearly vertical incidence and very gradual dispersion. No doubt in most areas low reflection coefficients in effect at the bottom of water layers prevent the development of this wave guide action. The example here described came to light through two special circumstances which favor real or apparent sustained reinforcement at practically constant amplitude level. First, over the seismic prospect which yielded the observations, the bottom of the water layer is smooth and

* Presented at the St. Louis meeting of the Society April 25, 1951. Manuscript received by the editor July 16, 1951.

† Geophysical Service Inc., Dallas, Texas.

‡ Lamont Geological Observatory, Columbia University, Palisades, New York. Contribution No. 34.

composed of rock, producing a high reflection coefficient even for normal incidence; second, automatic volume control on the amplifiers increases the gain for waves whose energy decreases due to leakage during a large number of reflections. This gives the impression of a long train of waves of almost constant amplitude.

Previous theoretical work can readily be extended to include the case of only partial reflection at the bottom. It will be shown that in this case there is a limiting frequency for which the group velocity approaches zero and the phase velocity approaches infinity. Normal mode propagation in simply the water layer produces seismograms showing waves which could easily be mistaken for a long series of excellent reflections from deep horizons.

OBSERVATIONS

Characteristic Seismograms

Since our introduction to the problem came through observation of seismograms on which regular reflection arrivals were obscured by water-transmitted energy, perhaps this discussion can be best introduced in a similar manner. Consider first then the seismogram illustrated in Figure 1, which may at first give the erroneous impression that it is a very good regular reflection record. The seismogram illustrates, among other things, the unusually long time throughout which wave amplitudes persist at levels that, because of automatic volume expansion, appear to be practically constant. Certain characteristics of the seismogram appear to repeat. A check on time intervals between them establishes periodicity. Further examination shows that almost every detail of trace movement is repeated over period after period. Essentially there is very little on the record beyond the features contained in a single interval such as the one indicated by marks.

Figure 2 shows a seismogram which, from the standpoint of seismic prospecting, is more obviously hopeless than the first and therefore less treacherous. This second seismogram is simpler, consisting mostly of a long train of nearly sinusoidal waves. It develops that Figures 1 and 2 involve the same pattern of propagation; they differ only in the particular normal modes present.

Empirical Formulas

Examination of a number of seismograms over a particular offshore prospect indicates frequency of this wave motion is closely related to depth of water. Trial shows the frequency formula

$$f = 3V/4H \tag{1}$$

describes the oscillations in Figure 2 well within the limit of accuracy with which water depth H is determined by sounding line or fathograms. Here V is velocity of sound transmission in water. In general, on many other records,

$$f = (2n - 1)V/4H \tag{2}$$

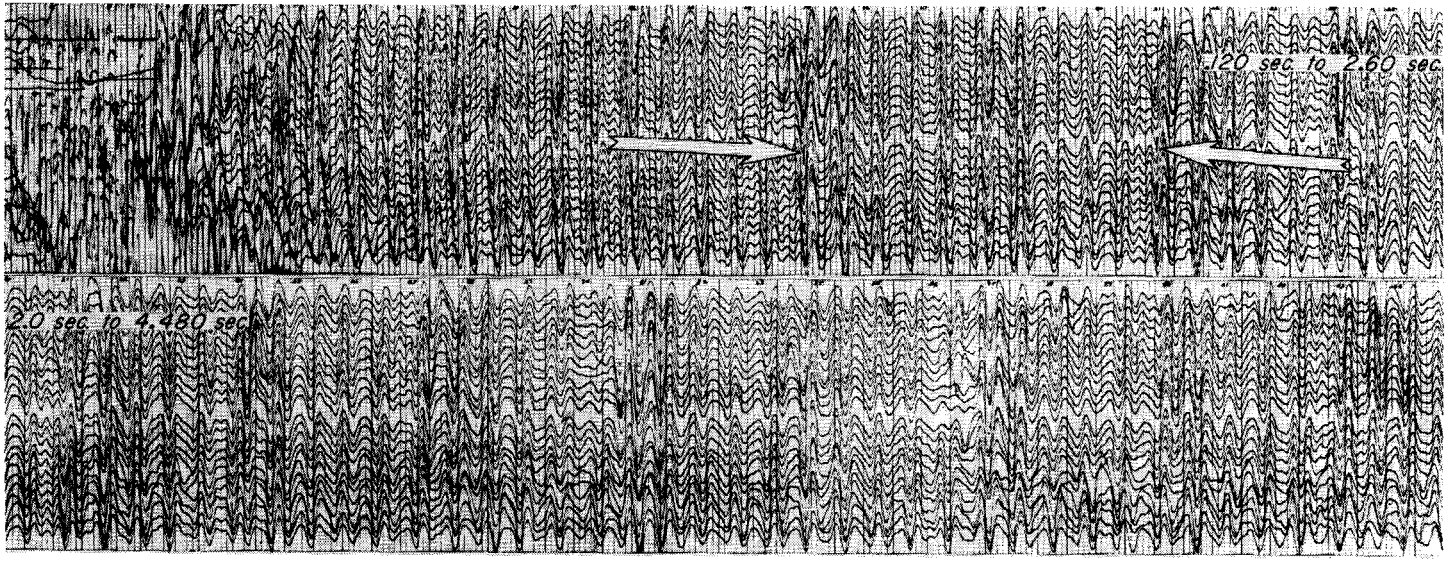

FIG. 1. 20 to 60 cycle per sec seismogram showing remarkable periodicity. Depths: Water, 148 ft; seismometers, 10 ft; 50 lb dynamite, 5 ft. Distances from shot: Trace 1, 1,090 ft; Trace 12, 665 ft; Trace 24, 1,285 ft. Recording spread: 2,000 ft.

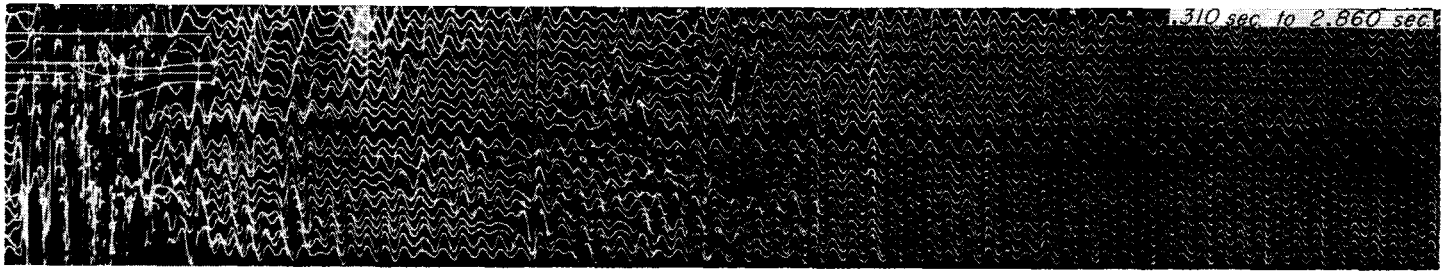

FIG. 2. 16 to 40 cycle per sec seismogram showing almost pure sine waves. Depths: Water, 132 ft; seismometers, 8 ft; 50 lb dynamite, 5 ft. Distances from shot: Trace 1, 2,405 ft; Trace 12, 2,155 ft; Trace 24, 2,340 ft. Recording spread: 2,000 ft.

where $n=1, 2, 3 \ldots$, fits the observations well. These are essentially the frequencies of resonance in vibrating bars clamped at one end or in organ pipes closed at one end.

Examples

Figure 3 shows a resonant record of relatively low frequency—about $22\frac{1}{2}$ cycles per second. Applying the formula for the second normal mode, $n=2$ in

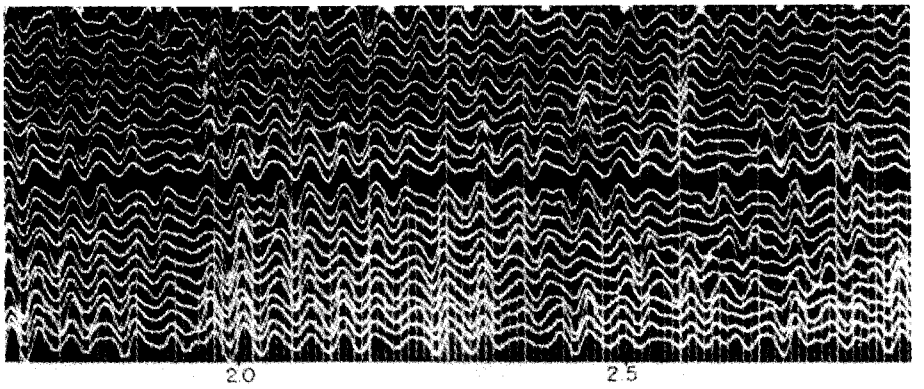

FIG. 3. 16 to 40 cycle per sec seismogram showing second odd harmonic or second normal mode of vibration. Depths: Water, 165 ft; seismometers, 8 ft; dynamite, 5 ft. Distances from shot: Trace 1, 2,555 ft; Trace 12, 2,275 ft; Trace 24, 2,480 ft. Recording spread: 2,000 ft.

Equation (2), and using 5,000 feet per second for propagation velocity gives $H=166$ feet. The fathometer reading was 165 to 167 feet. Figure 4 shows resonance in about 50 feet of water. Frequency here is 26.8 cycles per second. Computing depth, assuming the fundamental mode of vibration, gives 47 feet. Evidently the fourth normal mode appears in Figure 5; the 51 cycle frequency

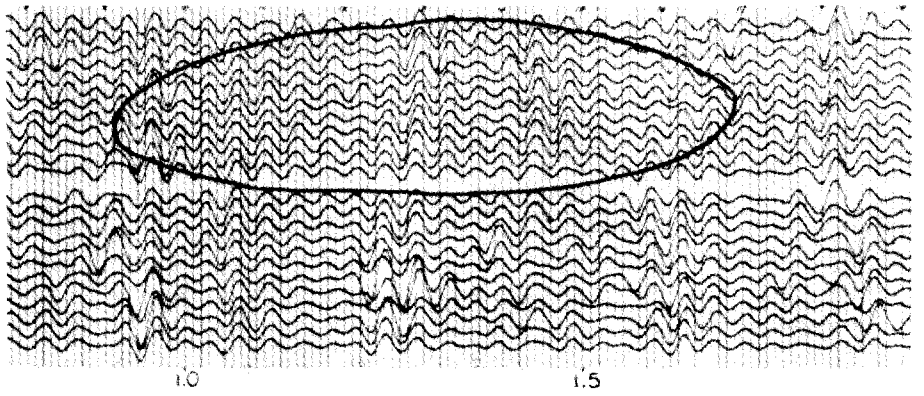

FIG. 4. 16 to 60 cycle per sec seismogram showing fundamental or first normal mode of vibration. Depths: Water, 53 ft; seismometers, 8 ft; dynamite, 5 ft. Distances from shot: Trace 1, 1,015 ft; Trace 12, 420 ft; Trace 24, 1,165 ft. Recording spread: 2,000 ft.

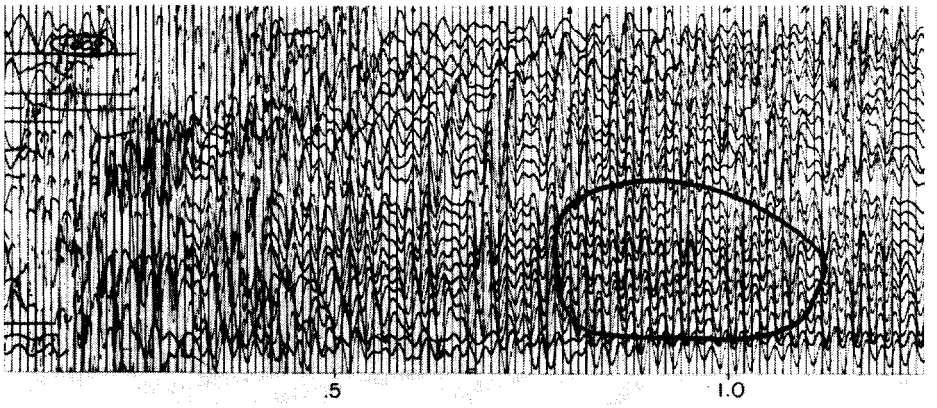

FIG. 5. 20 to 60 cycle per sec seismogram showing the fourth normal mode of vibration. Depths: Water, 164 ft; seismometers, 10 ft; dynamite, 5 ft.

applied in the appropriate formula gives 172 feet for H. The sounding records indicate a water depth of about 165 feet. In Figure 6 one finds the fifth normal mode. In deep water even extremely high frequencies recorded with wide pass

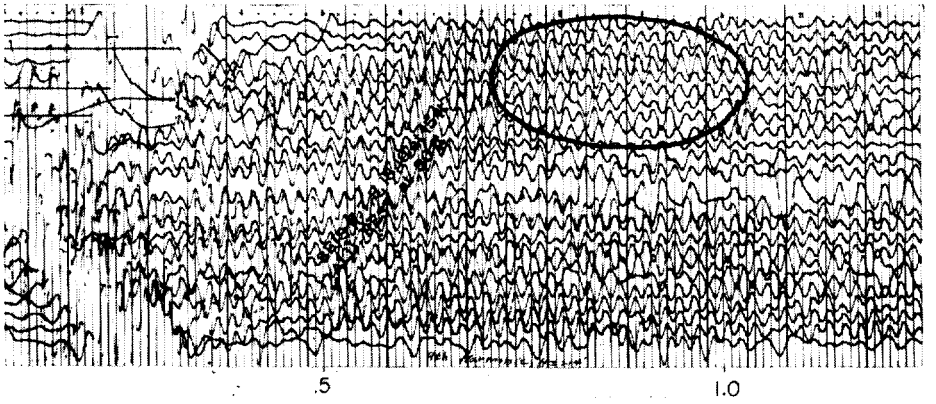

FIG. 6. 16 to 60 cycle per sec seismogram showing the fifth normal mode of vibration. Depths: Water, 214 ft; seismometers, 30 ft; dynamite, 214 ft. Distances from shot: Trace 1, 1,180 ft; Trace 12, 500 ft; Trace 24, 1,070 ft. Recording spread: 2,000 ft.

bands fit the resonance formula surprisingly well. In Figure 7 are shown sustained high frequency vibrations of many modes or harmonics. Recorded depth was 106 feet. Tentatively identifying an observed periodicity of 4.3 milliseconds with the eleventh normal mode and computing depth yields 113 feet.

As would be expected, the frequency response curves of our instruments determine roughly which modes appear. At least the range of frequencies that may be expected on a given seismogram narrows down to the limits of the pass band used. Although generally harmonics lying within the pass band are repre-

sented on a seismogram, it is sometimes difficult to account for the predominance of some and the absence of others. A typical frequency response curve appears in Figure 8. The arrow tips under the curve indicate a sequence of modes corresponding to the water depth above which the seismogram shown at the right was shot. On this record one can identify the third and fourth normal modes, which lie in the frequency range receiving optimum amplification.

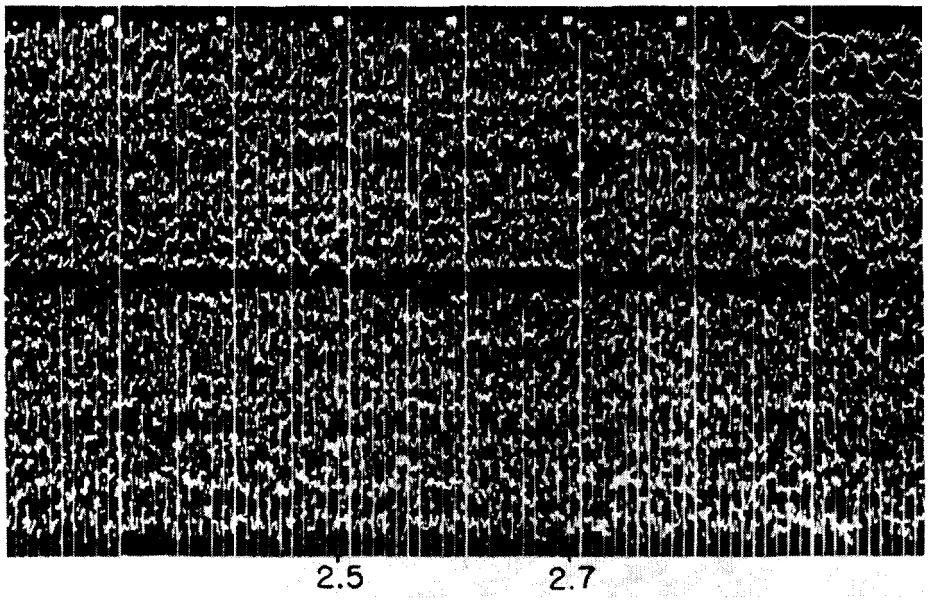

FIG. 7. Unfiltered seismogram showing various higher harmonics. Depths: Water, 106 ft; seismometers, 8 ft; dynamite, 5 ft. Distances from shot: Trace 1,2530 ft; Trace 12, 2,160 ft; Trace 24, 2,065 ft. Recording spread: 2,000 ft.

Figure 9 shows a portion of a seismogram obtained in 248 feet of water with a very flat uniform bottom. The cutout fitted to the top traces is a mathematically computed curve in which third, fourth and fifth normal modes were computed from the frequency formula and simply added. One can easily see that the curve applies almost equally well to any appropriate part of the seismogram segment shown.

THEORY

General Remarks

The unusually high multiples of reflections within the water layer offer evidence that reflection coefficients are close enough to unity so that even after many reflections their attenuating effect is substantially offset by an automatic increase in amplifier gain. Within the range of observations we have no specific data on amplitude level—only the illusion that oscillations continue practically

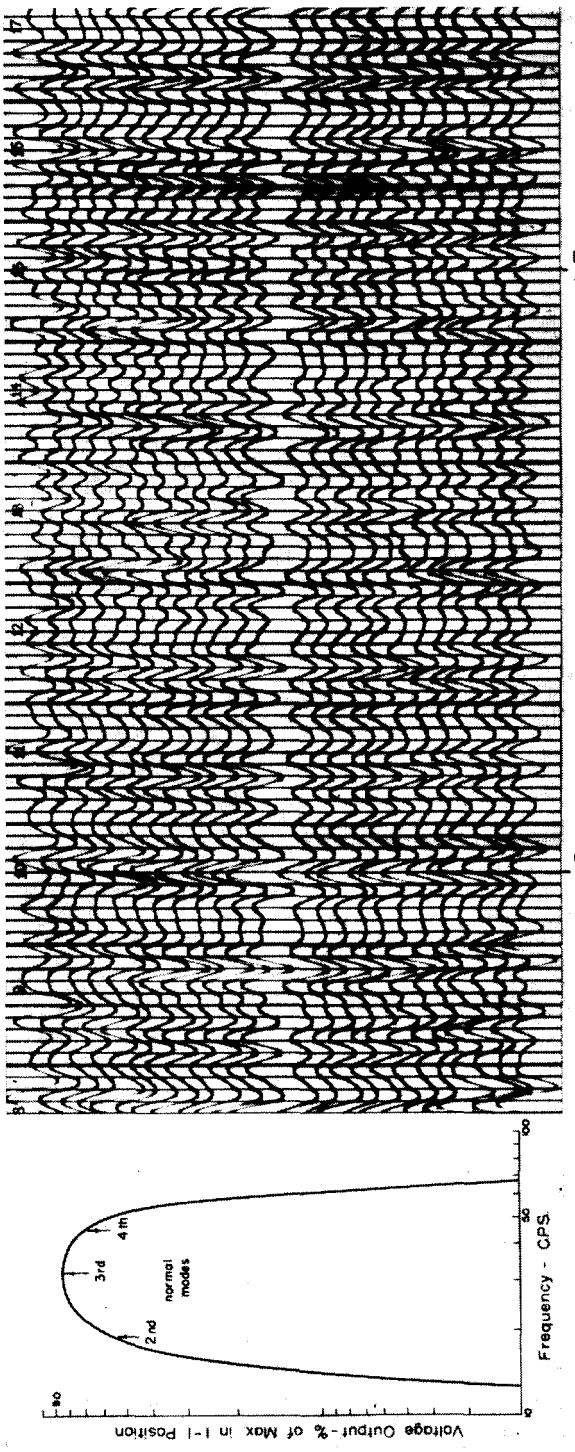

FIG. 8. Frequency response curve on a filter setting which on the seismogram at the right admitted third and fourth normal modes. Water depth: 192 ft.

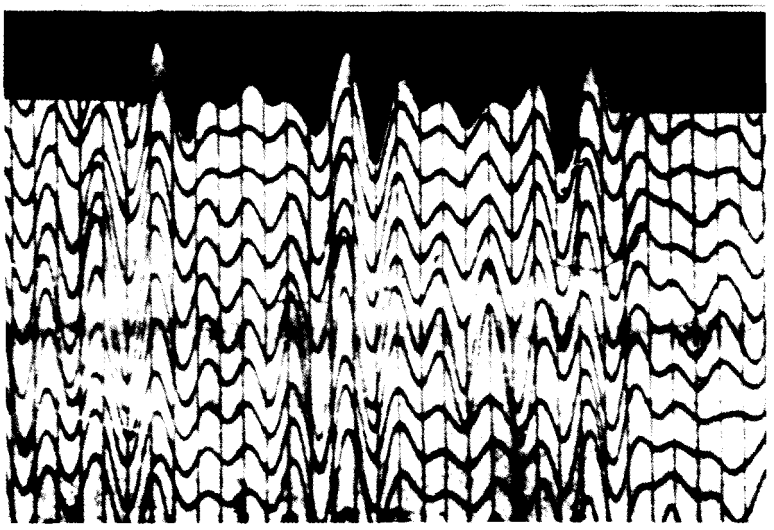

FIG. 9. The cutout at the top represents a mathematically computed curve of a combination of third, fourth, and fifth normal modes of vibration in water 248 ft deep. Note correlation with the actual seismogram below it.

undiminished. In first consideration of theory on an elementary level, then, the situation may as well be considered without reference to the effect of reflection coefficients, wave divergence, diffraction and other factors affecting attenuation.

Repetitive Arrivals of a Pulse

In this discussion we shall consider the shot a point source at (o, d) in an appropriately placed rectilinear coordinate system (x, z) with $z=o$ representing the surface of the water and $z=H$ representing a level bottom.

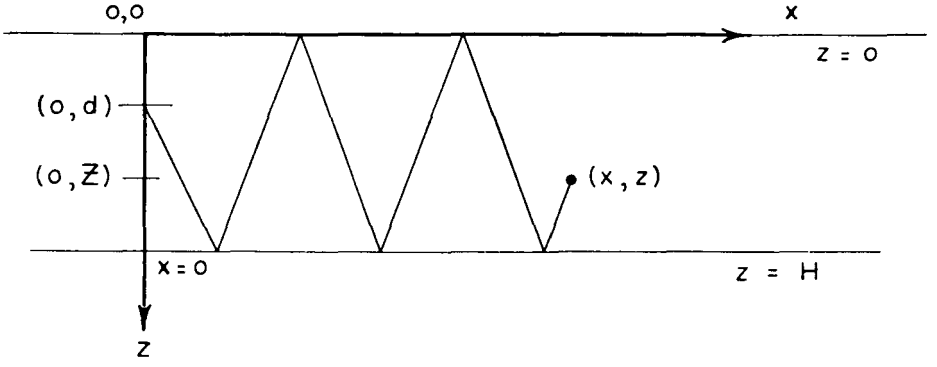

FIG. 10. Rays from (o, d) to (o, Z) multiple reflected at top and bottom of water layer and a particular ray path from (o, d) to (x, z) involving two reflections off the free surface.

Along $x=o$, a vertical line through the shot point, normal incidence applies upon reflection of the pulse at the boundaries of the water layer. It follows from the law of reflections that through successive reverberations the ray path of a pulse is here retraced repeatedly. A particular point (o, Z) in water H units deep therefore receives the pulse alternately from above and below until the energy dies down. See Figure 10.

Other points, (x, z) in general, are also bombarded by a succession of pulse arrivals from a single explosion, but the mechanics are somewhat different. A particular ray path applies at most only once, at a single instant of time. To present the matter in more detail, four types of propagation from (o, d) to (x, z) are shown in Figure 11. The classification is based upon the direction of the vertical component of wave front propagation initially at (o, d) and upon arriving at (x, z). Thus, P_d designates a ray which starts upward and passes (x, z)

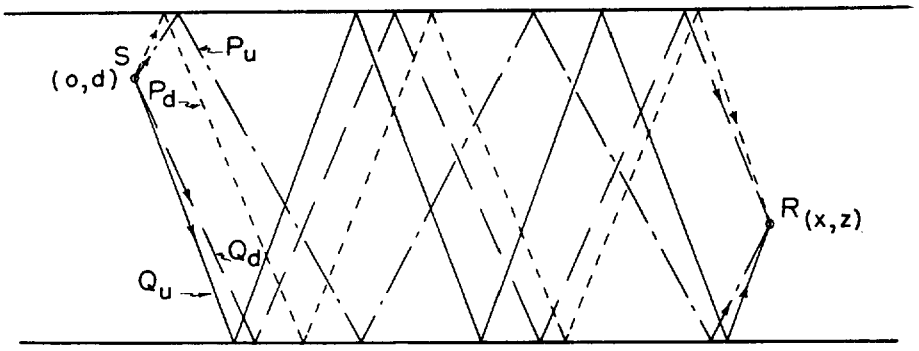

FIG. 11. Four types of ray paths from (o, d) to (x, z): P_d, initially upward, terminally downward propagation; P_u, initially upward, terminally upward; Q_d, initially downward, terminally downward; Q_u, initially downward, terminally upward propagation.

downward; P_u, a ray which starts upward and passes (x, z) upward; Q_d and Q_u represent rays which start downward and pass (x, z) downward and upward respectively. Thus, for a single pulse at (o, d) four not necessarily separate energy arrivals are indicated at (x, z) for any given number of reflections off the top. Furthermore, each of the four types of paths provides multiple arrivals in direct relation to the different number of reflections off the free surface.

Successive ray paths to (x, z) are indicated in Figure 12 for Q_d paths. If m denotes the number of reflections a given ray experiences off the top surface, it is apparent that the angle the ray makes with the vertical can be associated with the discrete number m and designated as $\theta_{Q_{dm}}$. Assuming a constant velocity of propagation V, path length is Vt where t is travel time, so this incident angle can be expressed in the two following ways:

$$\theta_{Q_{dm}} = \tan^{-1} \frac{x}{2mH - d + z} = \sin^{-1} \frac{x}{Vt}. \tag{3}$$

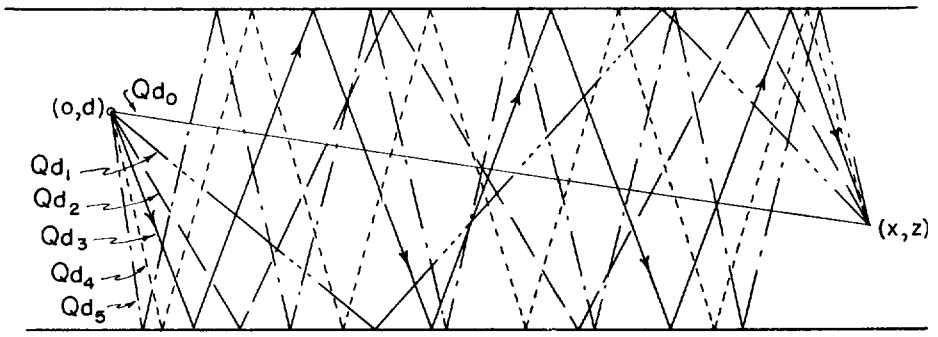

FIG. 12. The Q_d wave is schematically illustrated by ray diagrams for one through five reflections off the free surface between (o, d) and (x, z)—that is for $m=1, 2, 3, 4$, and 5 respectively.

Figure 12, as well as these expressions, shows convergence of successive rays through (x, z) toward the vertical as a limiting direction. $\theta_{m+1}-\theta_m$ thus becomes increasingly small. Ray length corresponding to $\theta_{Q_{dm}}$ is also $(2mH-d+z)\cos\theta_{Q_{dm}}+x\sin\theta_{Q_{dm}}$.

Since similar statements apply for the Q_{um}, P_{dm}, and P_{um} rays the situation may be summarized as follows:

Ray Designation	*Angle of Incidence*	*Travel Time*	*Path Length*
P_{dm}	$\theta_{P_{dm}}=\tan^{-1}\dfrac{x}{2(m-1)H+d+z}$	$t_{P_{dm}}=x/V\sin\theta_{P_{dm}}$	$Vt_{P_{dm}}=[2(m-1)H+d+z]\cos\theta_{P_{dm}}+x\sin\theta_{P_{dm}}$
P_{um}	$\theta_{P_{um}}=\tan^{-1}\dfrac{x}{2mH+d-z}$	$t_{P_{um}}=x/V\sin\theta_{P_{um}}$	$Vt_{P_{um}}=[2mH+d-z]\cos\theta_{P_{um}}+x\sin\theta_{P_{um}}$
Q_{dm}	$\theta_{Q_{dm}}=\tan^{-1}\dfrac{x}{2mH-d+z}$	$t_{Q_{dm}}=x/V\sin\theta_{Q_{dm}}$	$Vt_{Q_{dm}}=[2mH-d+z]\cos\theta_{Q_{dm}}+x\sin\theta_{Q_{dm}}$
Q_{um}	$\theta_{Q_{um}}=\tan^{-1}\dfrac{x}{2(m+1)H-d-z}$	$t_{Q_{um}}=x/V\sin\theta_{Q_{um}}$	$Vt_{Q_{um}}=[2(m+1)H-d-z]\cos\theta_{Q_{um}}+x\sin\theta_{Q_{um}}$

(4)

For any one of these four types of ray paths some convenient pulse characteristic, such as the extremes of pressure, plotted for successive arrivals at (x, z) with respect to time would appear somewhat as shown in Figure 13. A 180° phase shift with each reflection off the free surface requires that alternate arrivals be plotted below the axis.

Pulse Characteristics

In the case of the artificial seisms which produced the records previously shown, the origin of each disturbance was a dynamite explosion. The work of Cole and others indicates an underwater explosion of this type is propagated outward in the form of a pulse with roughly the shape illustrated in Figure 14, where pressure is indicated qualitatively with respect to time.

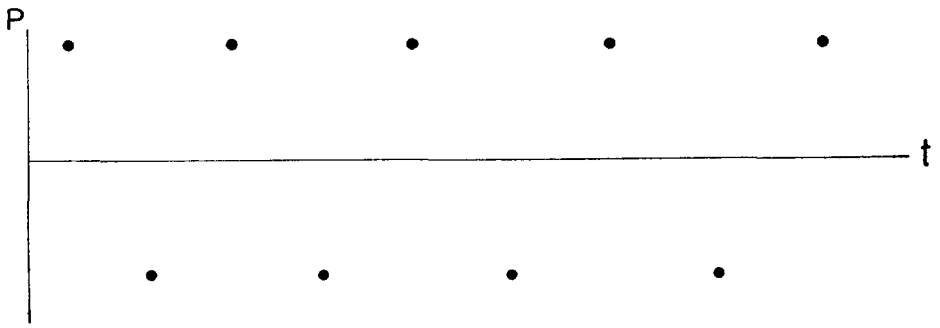

FIG. 13. Energy arrivals at (x, z) for a particular type ray for successively higher orders of multiple reflections. Pressure is plotted schematically with respect to travel time.

Experience and theoretical work by other writers indicates that this pulse is essentially a complex wave form representable by a continuous frequency spectrum of sine waves. In this discussion it will simply be assumed that the arrivals at any point (x, z) have the same general shape as the original pulse

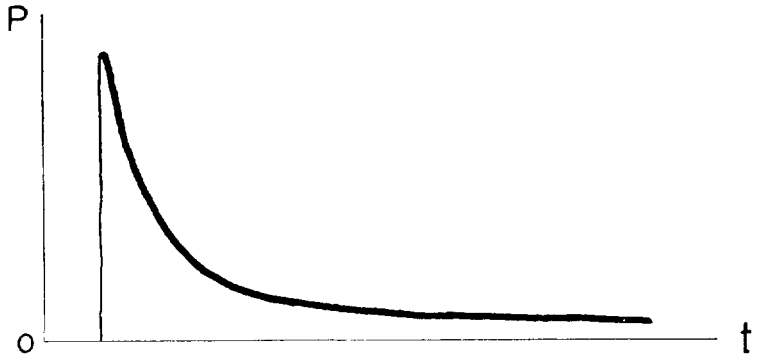

FIG. 14. Generalized pressure-time curve of an explosion.

for a few reflections—for small values of m. As m increases these arrivals are manifested by whatever frequency components are favored by interference effects between the multiply reflected waves and the frequency response of the recording system.

Wave Development

In line with this view on pulse characteristics one would then expect the multiple arrivals portrayed in Figure 13 to appear in the form of those wave components which fit the pulse arrival pattern. The lowest frequency range expected is shown fitted to these arrivals in Figure 15. Development of even harmonics of this wave will evidently be prevented by the alternations in phase.

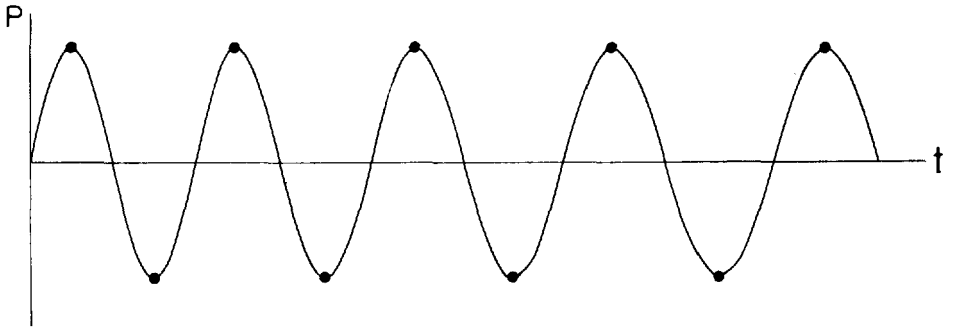

FIG. 15. Energy arrivals of Figure 13 fitted with an appropriate wave form.

Odd harmonics may, however, be fitted as well as the fundamental. The combination of eligible wave components may therefore be a quite complex wave form. Thus, Figure 9 shows the form developing out of the combination of three particular odd harmonics or normal modes. To investigate this wave development further let us express the four types of travel in the form of velocity potentials of the expected waves at any point (x, z) at a time t after m reflections from the free surface.[1]

$$\begin{aligned}
P_{dm} &= A(-1)^m\epsilon^{m-1} \exp i2\pi\{x \sin\theta + [2(m-1)H + z + d]\cos\theta - Vt\}/L,\\
P_{um} &= A(-1)^m\epsilon^m \exp i2\pi\{x \sin\theta + [2mH - z + d]\cos\theta - Vt\}/L,\\
Q_{dm} &= A(-1)^m\epsilon^m \exp i2\pi\{x \sin\theta + [2mH + z - d]\cos\theta - Vt\}/L,\\
Q_{um} &= A(-1)^m\epsilon^{m+1} \exp i2\pi\{x \sin\theta + [2(m+1)H - z - d]\cos\theta - Vt\}/L,
\end{aligned} \tag{5}$$

where $\theta = \sin^{-1} x/Vt$, L is the wave length measured along the oblique ray path, A is a variable amplitude factor which is left unevaluated, and ϵ is the bottom reflection coefficient depending on θ and the elastic properties of the two layers involved. Phase shifts during m reflections off the free surface are accounted for by the factor $(-1)^m$.

Let

$$\delta = \exp i2\pi(2H\cos\theta)/L = \exp i\pi(4H\cos\theta)/L. \tag{6}$$

Then

$$\begin{aligned}
P_{dm} &= A(-1)^m\epsilon^{m-1}\delta^{m-1} \exp i2\pi[x \sin\theta + (z + d)\cos\theta - Vt]/L,\\
P_{um} &= A(-1)^m\epsilon^m\delta^m \exp i2\pi[x \sin\theta - (z - d)\cos\theta - Vt]/L,\\
Q_{dm} &= A(-1)^m\epsilon^m\delta^m \exp i2\pi[x \sin\theta + (z - d)\cos\theta - Vt]/L,\\
Q_{um} &= A(-1)^m\epsilon^{m+1}\delta^{m+1} \exp i2\pi[x \sin\theta - (z + d)\cos\theta - Vt]/L.
\end{aligned} \tag{7}$$

[1] These wave expressions could, with minor modifications, be applied to direct analysis of other characteristics besides velocity potential, such as pressure, displacement, or vertical component of particle velocity.

The disturbance at any point (x, z) is due to the superposition of the various P and Q rays. Let us combine these as follows:

$$\begin{aligned} \Omega_d &= P_{d(m+1)} + Q_{dm} \\ \Omega_u &= P_{um} + Q_{u(m-1)} \end{aligned} \tag{8}$$

Ω may be thought of as the velocity potential due to the doublet source of the shot point and the image of its first reflection in the top surface. Carrying out the additions we obtain:

$$\begin{aligned} \Omega_d &= -A(-1)^m\epsilon^m\delta^m i \sin(2\pi d\cos\theta/L)\exp i2\pi[x\sin\theta + z\cos\theta - Vt]/L, \\ \Omega_u &= A(-1)^m\epsilon^m\delta^m i \sin(2\pi d\cos\theta/L)\exp i2\pi[x\sin\theta - z\cos\theta - Vt]/L. \end{aligned} \tag{9}$$

Constant factors have been included in the unevaluated factor A. Ω_d and Ω_u will both contribute to the disturbance at any one point. Their combined effect is $\phi = \Omega_d + \Omega_u$, or

$$\phi = A(-\epsilon\delta)^m \sin(2\pi d\cos\theta/L)\sin(2\pi z\cos\theta/L)\exp i2\pi[x\sin\theta - Vt]/L, \tag{10}$$

where constant factors have again been included in A.

The waves given by ϕ for m reflections interfere with those of ϕ for $m+1$ reflections. Reinforcement occurs if $\phi_m + \phi_{m+1}$ is a maximum or when the quantity $1-\epsilon\delta = 1-\epsilon\exp i2\pi 2H\cos\theta/L$ is a maximum. This condition is fulfilled for those wave lengths which satisfy the equation

$$2\pi 2H\cos\theta/L = (2n-1)\pi \tag{11}$$

where $n = 1, 2, 3 \ldots$ The wave length factor is then

$$L = (4H\cos\theta)/(2n-1). \tag{12}$$

Here the integer n determines the harmonic or the normal mode of propagation and the dependence of θ upon t establishes L as a function of t.

Since $\delta = -1$ under the condition for optimum wave development we may write

$$\phi_n = A\epsilon^m \sin\left(\frac{2\pi}{L} z\cos\theta\right)\sin\left(\frac{2\pi}{L} d\cos\theta\right)\exp i2\pi(x\sin\theta - Vt)/L. \tag{13}$$

With the aid of Equation 12 velocity potential can be written

$$\phi_n = A\epsilon^m \sin[(2n-1)\pi z/2H]\sin[(2n-1)\pi d/2H]\exp i2\pi(x\sin\theta - Vt)/L. \tag{14}$$

This expression represents a progressive wave traveling in the water layer in the x direction with dispersive characteristics, since $L = f(t)$, and with a standing wave pattern between the surface and bottom which is independent of θ. Nodal planes are consequently parallel to the surface. The summation of the velocity potentials ϕ_n for all modes, from $n = 1$ to ∞, and over as large a range of m as applies, gives the over-all disturbance at any point or instant of time. The

factor ϵ^m shows the effect of partial refraction into the bottom at each reflection.

A complete description of the resulting wave form would, of course, require a careful analysis of amplitude relationships embodied in $A\epsilon^m$. No record was kept of automatic volume gain expansion. A typical figure on volume control capacity is 10^5. Thus, while high amplitude particle motion arrives shortly after a shot, amplifier gain is throttled to the extent that trace motion on the seismogram may have an amplitude comparable with that produced by only 10^{-5} times as much particle motion with controls completely released. Since true amplitude ratios can be identified on observations only within limits as broad as this, and since elastic constants of the bottom were not measured, it was not considered worthwhile at this stage to identify expected amplitudes by theoretical expressions.

Dispersion Characteristics

The rate of progress of a particular phase is identifiable by the relation

$$\frac{d\frac{2\pi}{L}(x \sin\theta - Vt)}{dt} = 0. \tag{15}$$

Expressing L and θ in terms of x and Vt and differentiating $(v^2t^2-x^2)^{1/2}$ leads to the phase velocity expression

$$c = V/\sin\theta. \tag{16}$$

Group velocity measures the rate of progress of the wave group associated with each wave length. From simple geometry in this case, or from the general formula

$$U = c + Kdc/dK \tag{17}$$

where $K=(2\pi/L)\sin\theta$, one can identify group velocity as

$$U = V \sin\theta. \tag{18}$$

Since $\sin\theta=x/Vt$, we also have

$$U = x/t. \tag{19}$$

For each n or each normal mode of propagation frequency

$$f = V/L = (2n - 1)V/4H \cos\theta. \tag{20}$$

For reasons explained earlier we limit our discussion to values of θ in the range $\theta_c \geqq \theta \geqq 0$ where θ_c is the critical angle of reflection at the bottom, the angle with the vertical whose sine is the ratio of water velocity to the velocity of underlying material. The corresponding range of frequency is $f_c \geqq f \geqq f_0$ where f_c is the cutoff frequency beyond which the earlier theoretical discussions apply (see Pekeris or Press and Ewing, 1950) and f_0 is the cutoff frequency given by $(2n-1)V/4H$ for $\theta=0$. See Equation 2.

INTERPRETATION OF THEORY

An impulsive point source of sound in a water layer generates spherical waves which undergo numerous multiple reflections from the surface and a level bot-

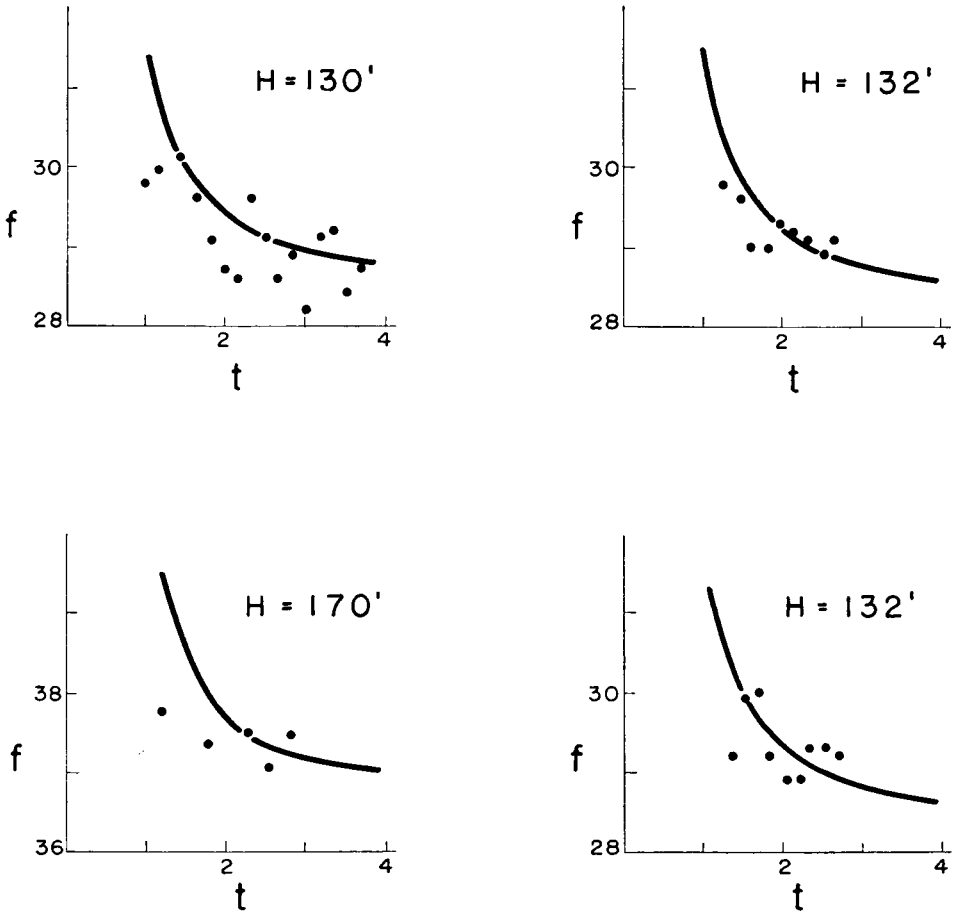

FIG. 16. Each graph shows wave frequency plotted with respect to arrival time for a particular record. Each plotted point represents an average of several actual observations. The smooth curves fitted to collections of average points represent the frequencies predicted by theory.

tom. The disturbance at any distant point is obtained by the superposition of all the waves arriving at this point by the different ray paths indicated.[2] The

[2] In fact a spherical wave can be represented by a sum of component plane waves with appropriate amplitude factors (Press and Ewing, 1950; Officer, 1951). Our elementary discussion can in a sense be considered an analysis of these plane waves leaving out the amplitude factor.

result of the combination is a single disturbance which travels outward from the source and vertically has a standing wave pattern of motion from the surface to the bottom.

The initial disturbance generated by an underwater explosion can be analyzed into a broad continuous frequency spectrum. However, only particular frequencies are reinforced according to normal mode propagation theory, and these are identified by Equation 20. Significantly, it is members of this set of frequencies that are observed. See Figure 16. Because these frequencies are a function of the incident angle θ, and in turn time t, for any particular x, they can be assigned characteristic velocities. The concepts of phase and group velocities were then introduced to distinguish between the velocity with which a constant phase proceeds and the velocity with which a given frequency proceeds forward.

A description of the system of waves associated with values of θ greater than the critical angle has been given elsewhere (Press and Ewing, 1950), where it was shown that the last waves of this group arrive at a time corresponding to propagation with a velocity of about 0.6 V. Following this group an infinitely long train of waves arrive associated with normal mode propagation for values of θ smaller than the critical angle. If one focuses attention on any given mode (by means of filters for example) the frequency of the waves decreases slowly with time, the rate of decrease becoming more and more gradual as time increases and as the cutoff frequency for $\theta = 0$ is approached. Phase and group velocity, however, are quite sensitive, approaching infinity and zero respectively as θ approaches 0.

These waves are attenuated due to partial refraction at each reflection from the bottom. For a given shot detector distance, the number of reflections m increases as θ decreases, hence attenuation due to reflection increases as travel time increases. For a given travel time and distance frequencies of the various modes have the ratios $1:3:5:7:\cdots$. To a large extent the resultant wave pattern actually recorded is determined by interference between the various modes admitted within the filter pass bands used.

The pressure or velocity field generated by an underwater explosion can be discussed most simply in terms of the pressure fields of the component normal modes. Expressions for pressure p or vertical particle velocity $\dot{w}$ can be derived from Equation (14) and the relationships

$$p = -\rho \frac{d\phi}{dt} \qquad \dot{w} = \frac{\partial \phi}{\partial z}.$$

Thus the vertical variation of pressure and particle velocity are respectively given by the factors

$$\sin\left[\left(\frac{2n-1}{2}\right)\pi \frac{z}{H}\right] \quad \text{and} \quad \cos\left[\left(\frac{2n-1}{2}\right)\pi \frac{z}{H}\right]$$

$$n = 1, 2, 3, \cdots. \qquad (21)$$

The following conclusions are evident from these equations:

(1) The surface $z=0$ is a nodal plane in pressure or an antinodal plane in vertical particle velocity for all frequencies and modes.

(2) The bottom $z=H$ is an antinodal plane in pressure and a nodal plane in vertical particle velocity for all frequencies in all modes.

(3) There are $n-1$ nodal planes in pressure for all frequencies and modes beneath the surface located at depths given by

$$\frac{z}{H} = \frac{2}{2n-1}, \frac{4}{2n-1}, \frac{6}{2n-1}, \cdots, \frac{2n-2}{2n-1} \quad n = 1, 2, \cdots.$$

(4) There are n nodal planes in vertical particle velocity located beneath the surface at depths given by

$$\frac{z}{H} = \frac{1}{2n-1}, \frac{3}{2n-1}, \frac{5}{2n-1}, \cdots, \frac{2n-1}{2n-1} \quad n = 1, 2, 3, \cdots.$$

The above equations would indicate that the response to these waves of a hydrophone sensitive to pressure changes and a geophone sensitive to vertical particle velocity varies with depth because of the vertical standing wave pattern. Since the ideal location of a detector for elimination of these waves is at a nodal plane, the preceding criteria may be used to determine theoretically the best depth for locating detectors. A similar discussion may be given for charge location.

MISCELLANEOUS ASPECTS

It must be obvious that the preceding remarks about the observed multiple reflection phenomenon are essentially introductory. Vital aspects of the problem have not been adequately treated. Of these, amplitude has already been mentioned.

A study of reflections from plates of finite thickness might disclose the possibility of a more detailed description of bottom conditions than given. A. B. Wood in *A Textbook of Sound* indicates thickness of the reflector is quite an important factor. Certainly a complete discussion of the problem would include a consideration of possible reverberation in shallow solid or semi-solid layers below the water.

Effect of corrugations along the bottom or top of the water layer has been entirely neglected. Nevertheless, a complete understanding of reinforcement phenomena would require more attention to this point.

In localities where the bottom is rugged no periodicity was observed. Even gently sloping bottoms must radically modify the described dispersion pattern or prevent the development of resonance altogether. Poulter's interesting analysis of slope determination from multiple reflection behavior appears to offer a promising approach to a study of the effect of bottom relief. The fact that parallel plates comprise only one example of electromagnetic wave guides or cavity

resonators suggests that seismic counterparts may not be restricted to the simple example here described.

The assumption that velocity of propagation is constant appears to be justified in our example by the close fit between observations and theoretical predictions. If dimensions of the region considered were radically altered, variations in propagation velocity might be pertinent factors.

Finally, this most excellent example of a seismic wave guide suggests that there may be others less perfectly developed. Numerous instances of periodicity on reflection records have been experienced in land shooting. Some may bear an interesting relationship to the reinforcement example herein discussed.

Establishment of a sound wave guide requires, in general, that

(1) A source of sound energy provide essentially true continuous wave motion or pseudo-continuous wave motion through pulse reverberation.

(2) Boundary geometry, transmission characteristics, and reflection characteristics be favorable to the development of particular reinforcement waves progressing away from the shot.

SUMMARY

Among the different types of waves observed in seismic measurements over water we can include the normal mode propagation produced by constructive interference as described in various papers by Ewing, Pekeris, and Press. A particular example of this type of wave develops relatively close to the source of energy provided bottom conditions are favorable. Seismograms from a particular prospect show this phenomenon so pronounced that all normal reflections from underlying beds are completely lost.

At the shot point the resonant condition which develops is analogous to that which develops in an organ pipe closed at one end. The geometry of spherical waves multiply reflected at the boundaries of the water layer provides for a spreading of the resonant zone out from the shot point. This progressive growth is accompanied by dispersion which takes the form of gradual changes in dominant frequencies.

Geometry and terminology of electromagnetic wave guides applies very nicely to this particular instance of normal mode propagation. The body of shallow water herein described might therefore be termed a leaking wave guide.

BIBLIOGRAPHY

Colin Cherry, *Pulses and Transients in Communication Circuits*, Chapter II, New York: Dover Publications (1950), 40–47; 59–76.

Robert H. Cole, *Underwater Explosions*, New Jersey: Princeton University Press (1948), 14–66; 110–146; 199–203; 231, 235, 236, 264.

Maurice Ewing, J. L. Worzel, and C. L. Pekeris, *Propagation of Sound in the Ocean*, Memoir 27, Geological Society of America (New York: 1948).

H. B. McCurdy, "Frequency Analysis of an Underwater Explosion," Thesis, Massachusetts Institute of Technology (1944).

C. B. Officer, Jr., "Normal Mode Propagation in Three Layered Liquid Half-Space," *Geophysics*, Vol. XVI, No. 2 (April 1951), 207–212.

T. C. Poulter, *Geophysical Studies of the Antarctic* (California: Stanford Research Institute, 1950), 46–81.

Frank Press and Maurice Ewing, "A Theory of Microseisms with Geologic Applications," *Transactions of the American Geophysical Union*, Vol. 29, No. 2 (April, 1948), 163–174.

———, "Low-Speed Layer in Water-Covered Areas," *Geophysics*, Vol. XIII, No. 3 (July, 1948), 404–420.

———, "Propagation of Explosive Sound in a Liquid Layer Overlying a Semi-Infinite Elastic Solid," *Geophysics*, Vol. XV, No. 3 (July, 1950), 426–446.

Lord Rayleigh, *Theory of Sound*, Vol. II, 2d ed. (New York: Dover Publications, 1945), 1–48 and Chapter XIII.

H. H. Skilling, *Fundamentals of Electric Waves* (New York: John Wiley & Sons, 1942), Chapters II, X, XIII.

A. B. Wood, *A Textbook of Sound* (New York: The MacMillan Company, 1930), 9–25, 56–69, 229–289, 313–317, 326–329.